

Novel Complex of Zinc (II) Dichloroethylenediamine: Synthesis, Characterization, *In-silico*, and *In-vitro* Evaluation against Cervical Cancer Cells

Indah Raya^{1*}, Desy Kartina², Ronald Ivan Wijaya¹, Rizal Irfandi^{3,4}, Eid A. Abdalrazaq⁵, Prihantono Prihantono⁶, Santi Santi⁷, Eka Pratiwi¹, Andi Besse Khaerunnisa¹, Dewi Luthfiana⁸, Bulkis Musa¹, Hasnah Natsir¹, Maming Maming¹, Zaraswati Dwyana Zainuddin⁹, Ramlawati Ramlawati¹⁰, Ahmad Fudholi^{11,12}, Andi Nilawati Usman¹³, Unang Supratman¹⁴, Maulida Mazaya¹⁵, Sandi Sufiandi¹⁶

Abstract

Objective: Cervical cancer is a malignancy originating from the cervix and often caused by oncogenic Human Papilloma Virus (HPV), specifically subtypes 16 and 18. Anticancer drugs are chemotherapeutic compounds used for cancer treatment. Therefore, this research aims to synthesize and characterize Zinc (II) dichloroethylenediamine (Zn(en)Cl₂) complex, as well as determine its antiproliferative activity against HeLa cells. The Zn(en)Cl₂ complex was successfully synthesized, and the antiproliferative activity was tested. **Methods:** The synthesis involved reacting ethylenediamine and KCl with Zn metal. The complex formed was characterized using a conductometer, UV-Vis spectroscopy, FT-IR spectroscopy, and XRD, while the activity was measured against HeLa cells. **Result:** The synthesis yielded a 56.12% conversion with a melting point of 198-200 °C and a conductivity value of 2.02 mS/cm. The Zn(en)Cl₂ complex showed potential activity against HeLa cells with an IC₅₀ value of 898.35 µg/mL, which was evidenced by changes in the morphological structure of HeLa cells. Its interaction with DNA targets was investigated by employing molecular docking. **Conclusion:** The observed data indicated that the Zn(en)Cl₂ complex bound to DNA at the nitrogenous base Guanine (DG) by coordinate covalent bonds. Interestingly, DG maintained interaction with the complex until the end of the docking simulation. Additionally, molecular dynamics (MD) simulation was conducted, and the results showed that Zn(en)Cl₂ remained bound to the DNA binding pocket all through the process.

Keywords: IC₅₀- HeLa cells- Zn(en)Cl₂- Molecular Docking- Molecular Dynamic

Asian Pac J Cancer Prev, **24** (12), 4155-4165

Introduction

Cervical cancer ranks as the fourth most frequently diagnosed cancer and the second most common in

Indonesia (Suryoadji et al., 2022), with up to 348,809 cases and a mortality rate of nearly 60% of the cases, accounting for 207,210 deaths (Agustiansyah et al., 2021). Cervical cancer cells are HeLa cells derived from

¹Department of Chemistry, Faculty of Mathematics and Natural Science, Hasanuddin University, Makassar 90245, Indonesia.

²Department of Chemistry, Faculty of Mathematics, and Natural Science, Universitas Pakuan Bogor, 16144 Indonesia. ³Department of Biology Education, Faculty of Teacher Training and Education, Universitas Puangrimanggalatung, Sengkang 90915, Indonesia.

⁴Department of Chemistry, Faculty of Mathematics and Natural Science, Universitas Negeri Makassar, Makassar; Jalan Daeng Tata Raya Makassar; 90244, Indonesia. ⁵Chemistry department, Faculty of Science, Al Hussein Bin Talal University, Ma'an- Jordan.

⁶Department of Surgery, Faculty of Medical, Hasanuddin University, Makassar; 90245, Indonesia. ⁷Medical Laboratory Technology, Faculty of Health Technology, Megarezky University, Makassar 90234, Indonesia. ⁸Bioinformatics Research Center, Indonesian Institute of Bioinformatics (INBIO), Malang, Indonesia. ⁹Department of Biology, Faculty of Mathematics and Natural Science, Hasanuddin University, Makassar 90245, Indonesia. ¹⁰Department of Natural Science Education, Faculty of Mathematics and Natural Science, Universitas Negeri Makassar, Makassar, Indonesia. ¹¹Solar Energy Research Institute, Universiti Kebangsaan Malaysia, UKM Bangi, Selangor 43600, Malaysia. ¹²Research Centre for Electrical Power and Mechatronics, Institute of Science (LIPI), Bandung, Indonesia.

¹³Midwifery Study Program, Hasanuddin University, Makassar, 90245, Indonesia. ¹⁴Department of Chemistry, Faculty of Mathematics and Natural Sciences, Universitas Padjadjaran, Jatinangor 45363, Indonesia. ¹⁵Research Center for Computing, Research Organization for Electronics and Informatics, National Research and Innovation Agency (BRIN), Cibinong Science Center, Jl. Raya Jakarta-Bogor KM 46, Cibinong 16911, West Java, Indonesia. ¹⁶Directorate of Laboratory Management, Research Facilities, and Science and Technology Park, Deputy for Research and Innovation Infrastructure - The National Research and Innovation Agency of The Republic of Indonesia

*For Correspondence: indahraya05@gmail.com

the abbreviation of Henrietta Lacks, who died in 1951 of cervical aggressive adenocarcinoma (Lucey et al., 2009). The predominant HPV genotypes in cervical carcinoma are 16 and 18, and the virus causes at least 70% of all cervical cancers (Bain et al., 2011).

Chemotherapy is one of the cornerstones of cancer treatment, and cytotoxic agents have been long applied as palliative treatment for metastatic disease (Cardoso et al., 2009; Deswati et al., 2020; Gong et al., 2010; Hadjiliadis and Sletten, 2009; Lancelotti et al., 2017). Cisplatin is a highly effective but highly toxic antitumor drug (Dorcier et al., 2006) used in several types of cancers, such as ovarian, testicular, and pulmonary cells (Avendaño and Menéndez, 2008). However, its side effects can initiate nephrotoxicity, neurotoxicity, and drug resistance (Li et al., 2019). Various transition metal properties and ligand combinations have led to a broad range of anticancer intercession, each with a unique mechanism of action (Li et al., 2019).

Molecules can interact with DNA to influence its transcription and replication, leading to apoptosis and cell death. The non-covalent interaction of metal complexes with DNA has highlighted the significance of nucleobase sequence recognition, recognition of various DNA conformations, and binding site selectivity in a minor or significant groove, mismatched nucleobase sites, and bulge loops. Furthermore, metal complexes with DNA sequence-selective and cleavage potential are required for extra anticipated applications (Li et al., 2019). For instance, $[\text{Au}(\text{en})_2]\text{Cl}_3$ has shown IC₅₀ data of 1-6 μM on prostate cancer cells (PC3). This golden ethylenediamine complex is recognized as an effective cytotoxic agent in prostate cancer cells, similar to cisplatin (Monim-ul-Mehboob, 2013).

Dithiocarbamate is an essential ligand used as an intermediate in chemical synthesis and a bioactive compound with outstanding applications in medicine, including activities such as anticancer, antibacterial, antitubercular, antifungal, anti-inflammatory, and anti-Alzheimer's disease. Recently, the dithiocarbamate moiety has been incorporated into numerous cores, namely, triazole and chalcone, to develop new hybrid compounds exhibiting *in vitro* or *in vivo* antiproliferative activities (Vila et al., 2022).

Zinc serves as a competitive inhibitor of Heme Oxygenase (HMOX1), which is produced in solid tumors (Huang et al., 2005). This metal has the ability to both cause apoptosis in some tumors and shield other cancer cells from apoptosis brought on by outside stimuli. Zn²⁺-mediated and induced ions facilitate the degradation of mutant proteins, leading to autophagy and cell death in cancer cell lines (Tsuneo, 2017). Additionally, Zinc plays an important role in various cellular processes, including proliferation, differentiation, and apoptosis (Guney et al., 2018).

Among the metal complexes, zinc (II) species was the most potent against all bacterial strains, with Zinc (II) derivatives presenting more significant activity than ampicillin and fluconazole (Yeo et al., 2021). Zn (II) cysteine dithiocarbamate covalently binds with DNA from cancer cells, leading to apoptosis (Irfandi and Prihantono, 2019). This complex was reported by Kartina et al., 2019

to be effective against mycobacterium tuberculosis and cancer cells. Therefore, the present research aims to synthesize a zinc complex with ethylenediamine ligands and evaluate its activity against the HeLa cancer cell line.

Materials and Methods

Materials

Zinc (II) chloride, Potassium Iodide, Potassium Chloride, Silver (I) Nitrate, ethylenediamine, Cisplatin, Roswell Park Memorial Institute Medium, DMSO, KBr, Ethanol (95%), Methanol (95%), Acetone (95%), Methylene chloride (95%), Chloroform (95%), n-hexane (95%), and Acetonitrile (95%) were the materials obtained from the Central Laboratories of Hasanuddin University and Padjadjaran University Bandung, Indonesia.

Synthesis of $\text{Zn}(\text{en})\text{Cl}_2$

To synthesize $\text{Zn}(\text{en})\text{Cl}_2$, 0.136 g (1 mmol) of zinc (II) chloride was dissolved in a small amount of water and 0.664 g (4 mmol) KI was added. Afterward, 1 mL of 1 M (1 mmol) ethylenediamine and 0.34 g of (2 mmol) AgNO_3 were introduced into the mixture. The deposits produced were filtered out, and the yielded filtrate was reacted with excess KCl and ethylenediamine. The filtrate was heated until solids formed, which were then filtered and dried.

Complex Characterization

Utilizing a UV-Vis spectrophotometer in the 200-700 nm region, the complex's electronic spectra were measured. An XRD analysis was used to establish the complex's crystal structure while infrared spectra were collected using a SHIMADZU spectrophotometer at 4000-300 cm^{-1} . Conductivity was measured with a conductometer, and the melting point was calculated using Electrothermal IA 9100.

Antiproliferative Activity Test on HeLa Cell Lines

The HeLa cells were treated with several concentrations of the $\text{Zn}(\text{en})\text{Cl}_2$ compound test solution, along with cisplatin as a positive control, and then incubated for 24 hours. The sample and dye reagent were then incubated for a further four hours at 37 °C. After adding a stop solution, the sample's ability to inhibit HeLa cells was counted using a multimode reader at maks (570–600 nm). By extrapolating a 50% line of positive control absorption on the absorption curve in relation to various sample concentrations, the IC₅₀ values were determined.

Research Methods

Molecular Docking of $\text{Zn}(\text{en})\text{Cl}_2$ complex to Target DNA of Breast Cancer Cells

Basic validation of the PLANTS protocol

Protein and ref_ligand (reference ligand) preparation was carried out using the YASARA software (Zhang et al., 2003), by removing unwanted ligand and protein parts.

The ligand was prepared at pH 7.4 with MarvinSketch and saved as ligand_2D.mrv. The structure was then optimized by searching for different conformations using "Conformers search" in MarvinSketch, and the results were stored as a ligand with file.mol2.

The PLANTS software was employed to dock the prepared ligand and protein structures, with the input files in protein.mol2 and ligand.mol2. The docking pose that had the highest score was identified as the original position of the ligand in the target protein structure. It was further evaluated by performing RMSD (Root Mean Square Deviation) calculations using YASARA. The protocol was deemed valid once the RMSD value of the docked pose was less than 2 Å (1 Å = 10⁻¹⁰ m).

Molecular Dynamics Simulation

To clarify the stability of the protein-ligand and structural flexibility of protein, molecular dynamics simulation was performed using YASARA v22.9.24.W.64 software over period of 20.00 nanoseconds with timestep of 2.0 fs and AMBER14 force field (AMBER14 is one of the force field parameter and potential packages used in molecular simulations. In the case of YASARA DYNAMICS, the AMBER14 force field serves as a mathematical guide that describes the interactions between atoms and molecules in the simulated system). Before the simulation process began, the parameters were setting out in the md_run.mcr script (md_run.mcr is the name of the script file used in YASARA DYNAMICS software to carry out molecular dynamics simulations). The simulation was carried out at a physiological temperature of 310K or 37°C and 1 atmospheric pressure. The amount of sodium chloride is fixed at 0.9% to preserve the sample's viability under the physiological condition. The physiological pH of the body was also represented by the pH 7.4 treatment. After the macro script's parameters were established, the software application performed it.

Running md_analyze.mcr and md_analyzebindenergy (script files used in molecular dynamics simulations to analyze the data generated from the simulation). This data produces a report with potential energy, RMSD, number of hydrogen bonds in the solute, and binding energy values. Running md_play.mcr enabled a more detailed presentation of snapshots at each simulation time, and Biovia Discovery Studio Visualizer and Chimera 1.16 were used for molecular visualization.

Results

Based on the results, the Zn(en)Cl₂ complex had a great yield of 56.12%, indicating a strong coordination bond between the metal and ligands which was supported by high melting points of 198-200 °C. The high melting points showed that the ligands were strongly bonded to the metal. Also, the measured conductivity value of 2.02 mS/cm suggested the Zn(en)Cl₂ complex as a non-electrolyte compound (Figure 1).

UV-Vis Characterization

An increase in the maximum wavelength value of ethylenediamine observed in the complex was attributed to the absence of electron donors between ethylenediamine and zinc (II). The resulting transition was $\pi \rightarrow \pi^*$ with a maximum wavelength of 233 nm (Figure 2).

IR characterization

The infrared absorption spectrum showed peaks at 511 and 509 cm⁻¹, providing evidence of a reaction between the metal and ethylene ligands. Additionally, the spectrum

Table 1. The Average Value of Total Potential Energy of the Complex System

Complex	Minimum and Maximum (kJ/mol)	Average (kJ/mol) ± Std
DNA-free (control -)	(-304.410) - (-248780)	-250.238 ± 6.107
Cisplatin-DNA (control +)	(-305.996) - (-246.130)	-247.788 ± 6.622
Zn(en)Cl ₂ -DNA	(-305.400) - (-244.877)	-246.624 ± 6.558

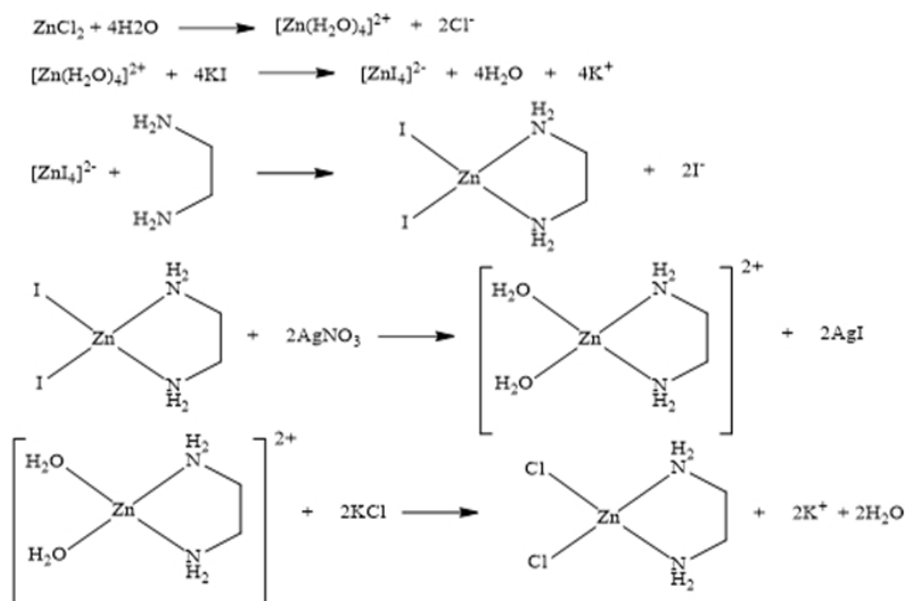


Figure 1. Synthesis Reaction of Zn(en)Cl₂ Complex

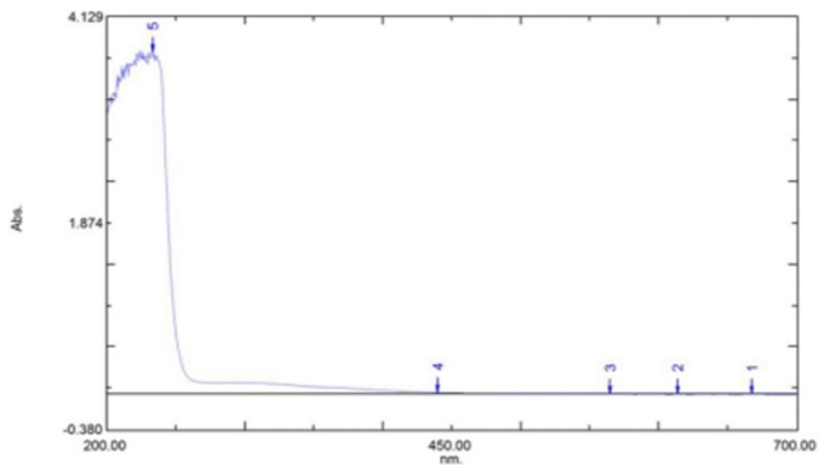


Figure 2. UV-Vis Spectrum of Zn(en)Cl₂ Complex

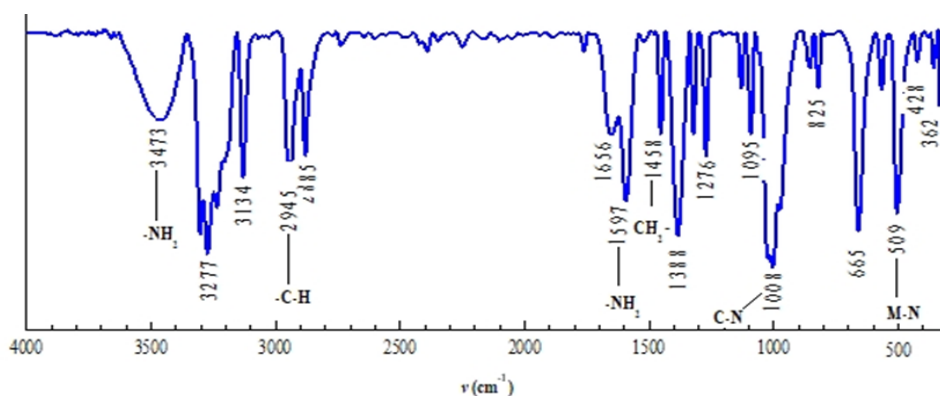


Figure 3. IR Spectrum of Zn(en)Cl₂ Complex

indicated the absence of ethylenediamine by exhibiting the presence of -NH₂, -CH₂-, and C-N groups at 1597, 1458, and 1008 cm⁻¹ wavelengths, respectively (Figure 3).

XRD characterization

The purpose of XRD characterization of the synthesized product was to ascertain the crystalline structure of the

Table 2. RMSD C-alpha Values of the Complex

Complex	Minimum and Maximum (Å)	Average (Å) ± Std
DNA-free (control -)	0.48-2.09	1.50 ± 0.27
Cisplatin-DNA (control +)	0.70-4.97	3.87 ± 0.74
Zn(en)Cl ₂ -DNA	0.62-5.86	4.41 ± 0.70

Table 3. RMSD Ligand Movement Values of the Complex

Complex	Minimum and Maximum (Å)	Average (Å) ± Std
Cisplatin-DNA (control +)	1.99-6.04	4.52 ± 0.83
Zn(en)Cl ₂ -DNA	1.74-6.30	4.15 ± 0.80

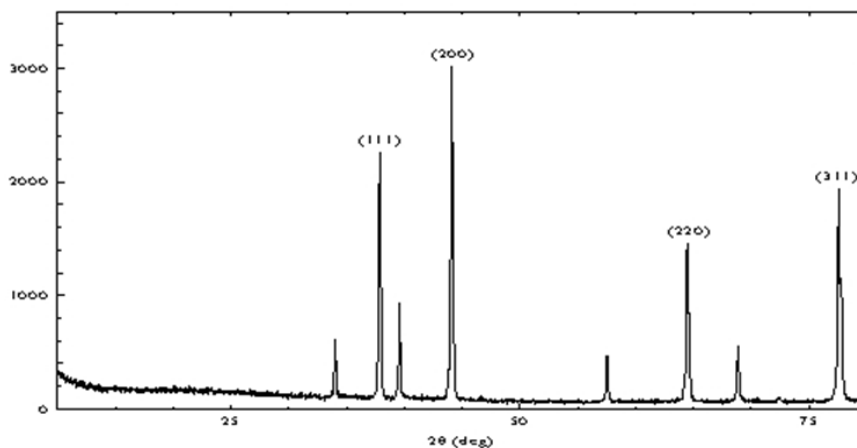


Figure 4. XRD Spectrum of Zn(en)Cl₂ Complex

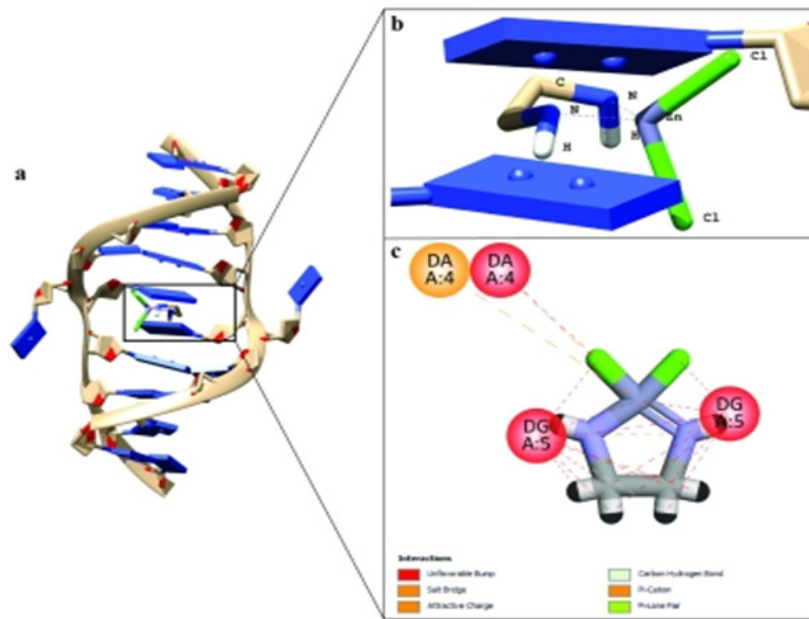


Figure 5. Representative Interaction of the $Zn(en)Cl_2$ Complex with DNA (PDB 1DDP) Using Chimera 1.16, b) $Zn(en)Cl_2$ complex interaction pathway with DNA, c) Representative interaction of the $Zn(en)Cl_2$ complex with DNA (PDB 1DDP) using VDS

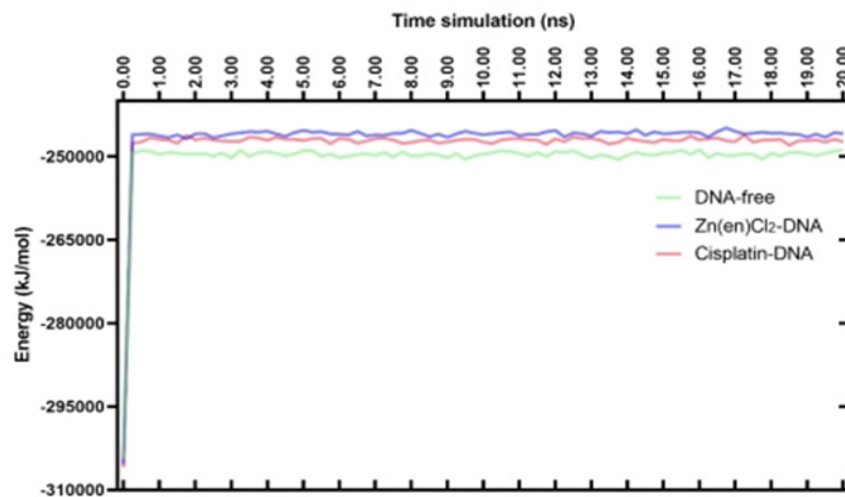


Figure 6. The Graph of Total Potential Energy of the Complex System during the Simulation Process

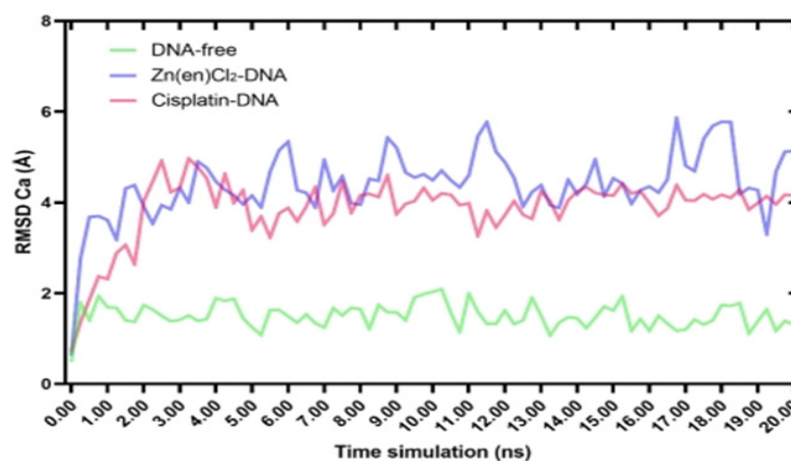


Figure 7. The RMSD C-alpha Values of the Complex for 20 ns

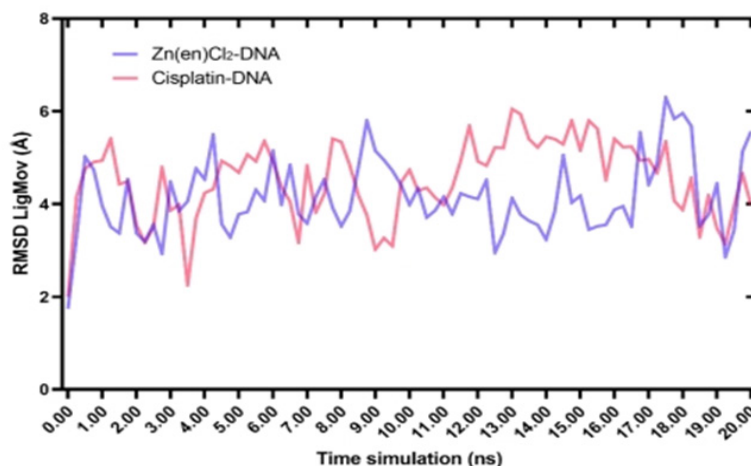


Figure 8. The RMSD Ligand Movement Values of the Complex for 20 ns

complex compound. The diffractogram obtained from the characterization indicated Miller indices that can be used to determine the crystal structure. The analysis results showed a face-centered cubic (FCC) crystal structure. The highest intensity diffraction angles (2θ) were 37.83, 44.07, 64.44, and 77.55 degrees (Figure 4).

Molecular Docking with DNA

Molecular docking is a structure-based computer-

aided drug discovery method serving as a powerful tool for generating hypotheses based on ligand binding poses and detailed predicted ligand/protein interactions that guide the designing of improved small molecules. It is crucial for computational ligand docking methodologies to successfully identify and confirm protein-ligand interactions. In this research, molecular docking calculations were employed to investigate the interaction between the $Zn(en)Cl_2$ complex as a potential new drug and DNA (Nyarko et al., 2004). Generally, molecular docking techniques suggest the most acceptable mechanism for intermolecular interactions between drugs and biomolecules. The result of the docking model revealed that the $Zn(en)Cl_2$ complex interacted with the DNA through intercalation mode. According to Figure 5,

Table 4. Average MM/PBSA Value for the Complex

Complex	MM/PBSA (kJ/mol) \pm Std
Cisplatin-DNA (control +)	-16.176 \pm 2.588
$Zn(en)Cl_2$ -DNA	-562.466 \pm 193.237

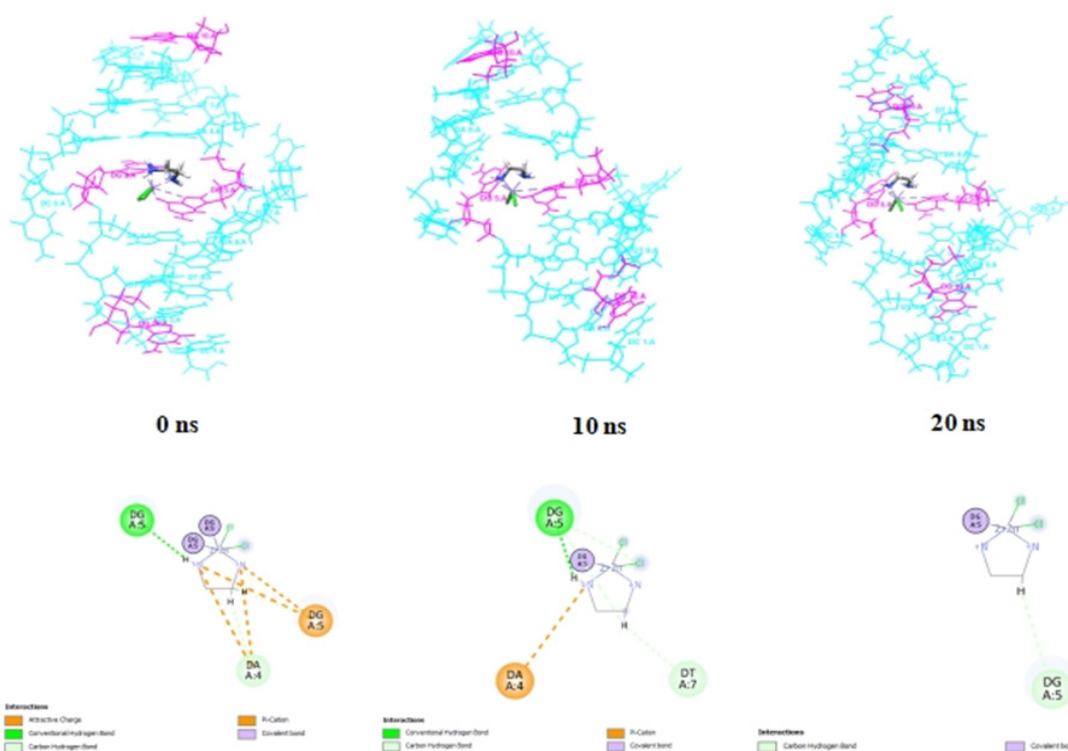


Figure 9. The Molecular Interaction between $Zn(en)Cl_2$ at the DNA Binding Site after Equilibration Process (left), 10 ns (center), and 20 ns (right) in the molecular dynamic simulation

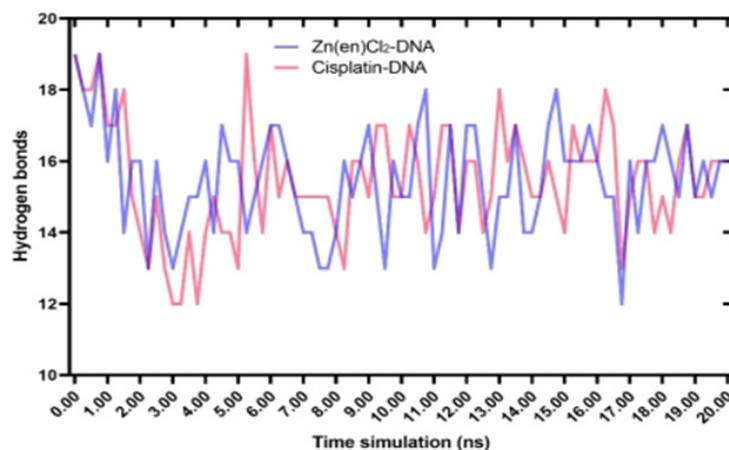


Figure 10. Number of Hydrogen Bonds of the Complex during Simulation

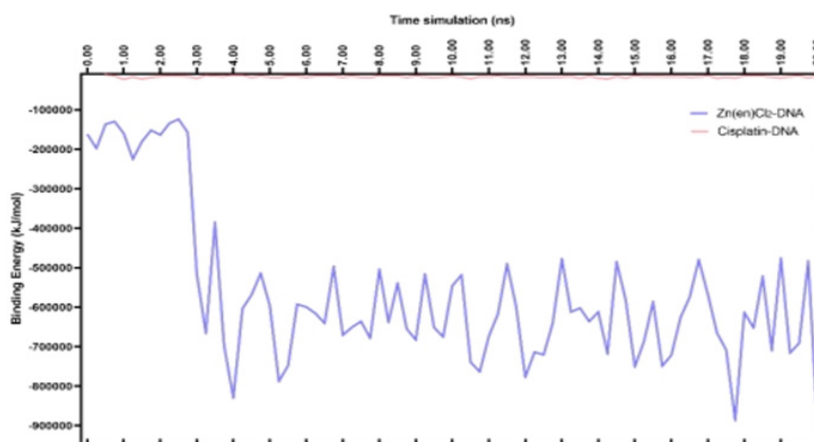


Figure 11. The Binding Energy Values of MM/PBSA of the Complex during the Simulation Process

the complex fitted in between the DNA nucleotides without rupturing the DNA double helix. Furthermore, it formed coordinate covalent bonds with DG and interacted with DNA base pairs through van der Waals forces. The complex engaged in π - π stacking with adenine base pairs (DA and DA: A4) and formed hydrogen bonds with DG by interacting with π - lone pair bonds (Ghosh, 2007).

Molecular Dynamics Simulation

In computational drug discovery, MD is often used to

simulate the ligand and receptor with varying temperature and time that mimics wet experiments (Durrant and McCammon, 2011; Nair and Miners, 2014). Moreover, it is beneficial to deep understanding the ligand binding at the binding site of the target protein (Salo-Ahen et al., 2021). In this study, MD was performed to understand the dynamic behavior and the structure stability of the ligand-DNA during the simulation. To investigate the binding of two metal complexes-based anticancer drugs, this study analyzed the potential energy, RMSD C-alpha,

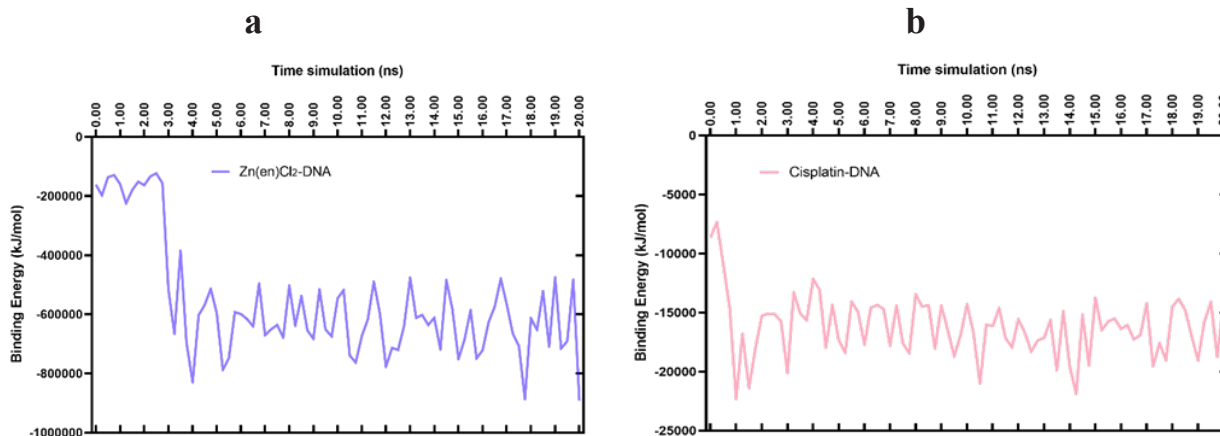


Figure 12. a) Binding energy of Zn(en)Cl₂-DNA b) Binding energy of Cisplatin-DNA

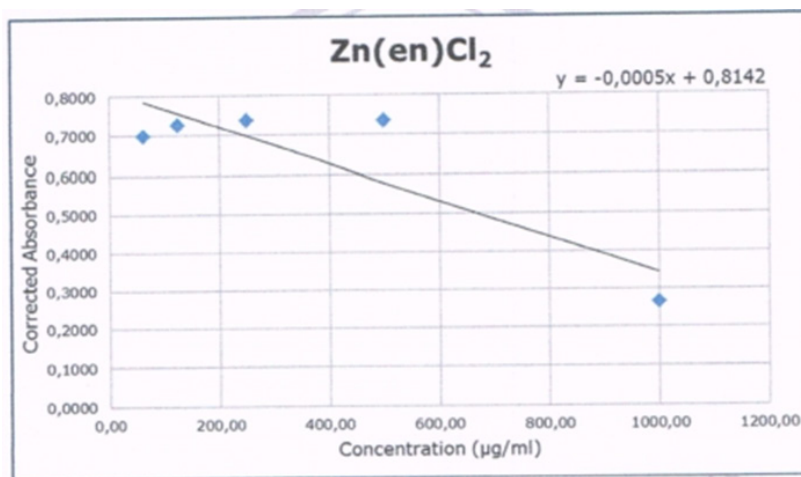


Figure 13. Curve of Zn(en)Cl₂ Antiproliferative Activity Test against HeLa cells

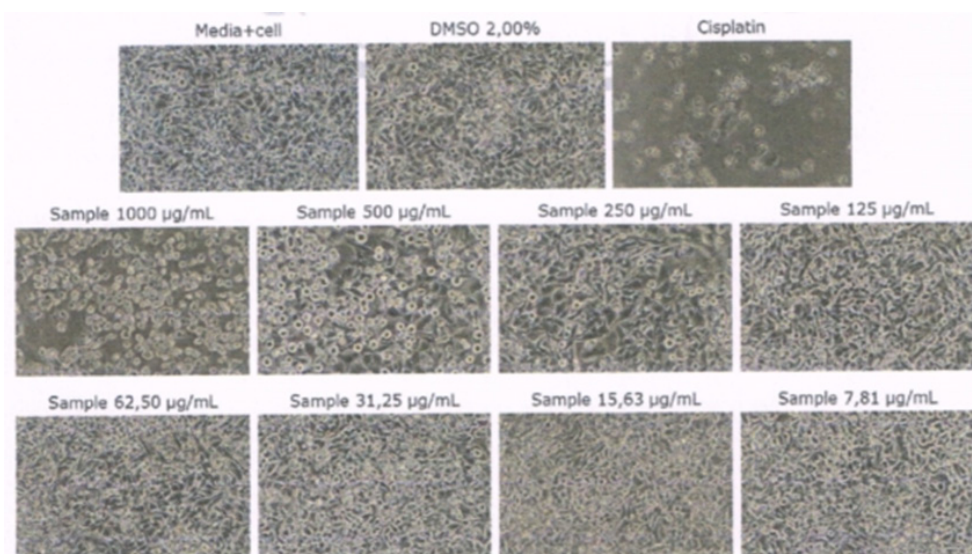


Figure 14. Apoptosis of HeLa Cells Induced by Zn(en)Cl₂ Complex

RMSD ligand movement, and binding energy calculations of Cisplatin-DNA (as a control positive) and Zn(en)Cl₂-DNA which are shown in Figure 6, Figure 7, Figure 8, Figures 10, and Figure 11 respectively. The results are also complemented with the detailed Table as illustrated in Table. 1, Table. 2, and Table. 3, and Table. 4.

Potential Energy

Potential energy defined as the sum of all bond

energies, bond angle energies, dihedral angle energies, planarity, van der Waals energies, and electrostatic energies (Irfandi et al., 2023). To evaluate the structural quality of protein, potential energy can be calculated based on the results of energy, angle, and planarity of protein (YASARA, 2023).

As shown in Figure 6., there is a sharp increase in energy during the first nanoseconds due to partly of the added kinetic energy is stored as potential energy. When

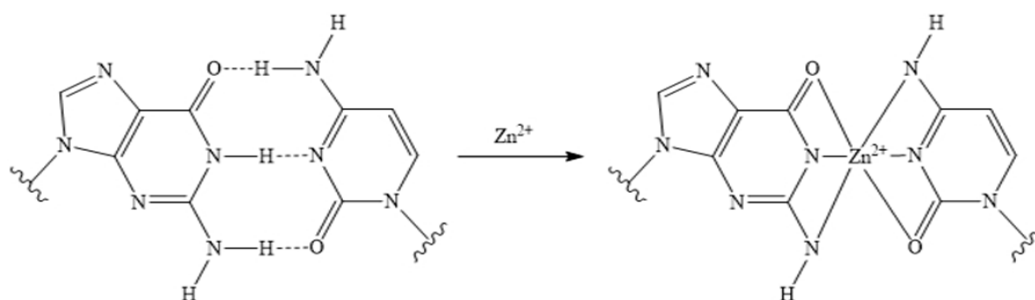


Figure 15. The Reaction of the Zn(en)Cl₂ Complex with N(7) Guanine (the Constituent Part of DNA)

a time scale is larger, the potential energy will frequently not decrease due to the present of counter ions. Initially, these are placed in the areas with the lowest potential energy, mainly near charged solute groups, from which they detach to obtain entropy and potential energy. The result illustrated that Zn(en)Cl₂ complex has similar trend to DNA-free and cisplatin, so it indicates that the complex is stable during the simulation.

Discussion

To understand the conformational change of DNA during the simulation, RMSD C α was analyzed in this study. The graph of RMSD C-alpha value of the complex during simulation time of 20 ns is presented in Figure 7, while Table 2, shows the calculation of RMSD C-alpha. RMSD value in molecular dynamics is used to compare the stability of a protein structure throughout the simulation (Martínez, 2015). This study used DNA-free as a control negative which was considered as the undamaged DNA and Cisplatin as a control positive. The indicator of RMSD value less than 3Å is used to determine the stability of the ligand-protein complex. In detail, to clarify the stability of the complex based on the RMSD value, we utilized the difference value term of both complexes compared with DNA-free (Cisplatin: 2.37Å, Zn(en)Cl₂: 2.91Å). According to the Figure 7, although the trend of the Zn(en)Cl₂ complex more fluctuated than Cisplatin, the RMSD difference value does not exceed the threshold value of 3Å. The result suggests that ligand Zn(en)Cl₂ is not disrupting the stability of DNA, but the presence of the ligand can increase the stability of DNA. Moreover, Zn(en)Cl₂ fairly bound to the binding site of the DNA during the simulation. The higher RMSD value of the complex, the more unstable the drug-DNA structural quality upon ligand binding, so the RMSD with the lowest value is preferred due to the minimal structural change during the simulation (Jalili et al., 2016).

As part of RMSD C-alpha, this study also examines the RMSD value of ligand movement. This aims to understand the movement of the ligands in the binding pocket during the simulation. The high value of RMSD ligand movements indicate that the ligand position is away from the binding site, then using this simulation the stability of the complex in DNA binding site can be investigated. As shown in the Table 3. the average value of the RMSD ligand movement of Zn(en)Cl₂ (4.15Å) and Cisplatin (4.52Å) are almost equal. This condition illustrates that the Zn(en)Cl₂ complex remains bound at the binding pocket of DNA at various time intervals, as cisplatin as does. When the movement is far away, it indicates major deviations in ligand from starting points. These results are also supported by the visual illustrations as shown in Figure 9 at different time intervals.

The molecular interactions of the complex before and after the MD simulation are shown in Figure 9. In accordance with Figure 9, the ligand continued to engage with DG through covalent bond contact, pi-pi interaction, and hydrogen bond interaction as the DNA-Zn(en)Cl₂ complex transitioned from the equilibration stage into the production stage (0 ns). In addition, the hydrogen bond

interaction between the ligand and two nucleotides (DA and DT) was also noticed. Curiously, DG continued to interact with the ligand up until the simulation's finish. The outcome of the MD simulation shows that Zn(en)Cl₂ remained bound to the DNA's binding pocket throughout the duration of the simulation.

To understand the change of DNA structure upon binding to ligand, hydrogen bond calculation should be considered. Over the simulation, DNA is stabilized by hydrogen bonds, so the significant decrease of hydrogen number indicate that its structure is less stable. According to the Figure 10, it reveals that both metal complexes have equal number of hydrogen bonds with slightly decrease from its initial condition. The results indicate that the ligand binding to DNA does not significantly affect the double strand structure of DNA during the simulation.

To calculate the binding energy value of the metal complexes, this study used MM/PBSA method. It is a computational method combined with molecular mechanical energy and a model of complex solution (Awaluddin et al., 2021). The binding energy in the simulation was calculated according to the equation:

$$\text{Bind energy} = E_{\text{potReceptor}} + E_{\text{solvReceptor}} + E_{\text{potLigand}} + E_{\text{solvLigand}} - E_{\text{potComplex}} - E_{\text{solvComplex}}$$

The results from binding energy of each complex are averaged to obtain the MM/PBSA binding energy values. The positive value of binding free energies shows that the binding of the metal complexes to DNA in water is favorable. According to the results, it is illustrated that Zn(en)Cl₂ complex has less ability to bind to DNA than cisplatin, so Zn(en)Cl₂ is less favorable in the simulation. The high difference value between Zn(en)Cl₂ and cisplatin may reveal that DNA is not the suitable target of Zn(en)Cl₂. Even though there is an interaction of the ligand to the binding site of DNA until the end of simulation, it might be not as strong as cisplatin does.

Based on Figure 12, the curve equation was determined to be $y = -0.0005x + 0.8142$ for the Zn(en)Cl₂ complex antiproliferative activity test conducted against HeLa cells. Furthermore, the IC₅₀ value was calculated by substituting y with 50, yielding 898.35 µg/mL. The observed antiproliferative activity of the complex was probably due to its metal bioactivity in the HeLa cells and the complex structure formed. The antiproliferative activity results in Figure 13 showed that the Zn(en)Cl₂ complex treatment could induce cell death or apoptosis in HeLa cells. The level of cell death was directly proportional to the concentration of the test compound administered to the HeLa cell suspension.

According to Figure 14, the Zn(en)Cl₂ complex bound to DG and coordinated a covalent bond with DNA double helix, allowing the metal Zn ion to form a cross-link between the two DNA strands. This cross-linking prevented cell division during the mitosis process, leading to the cessation of tumor growth (Irfandi Raya et al., 2022; Irfandi et al., 2023; Irfandi et al., 2022; IrfandiS Santi et al., 2022). Furthermore, tumor cell stiffness induced by cross-linking of Zn(en)Cl₂ could cause irreparable DNA damage and cell apoptosis (Figure 15). This research highlighted the potential of using essential metals as complexes to be tested for their

anticancer activity against HeLa cells.

In conclusion, The Zn(II)dichloroethylenediamine complex synthesized and characterized in this research exhibited promising anticancer activity against HeLa cancer cells, thereby indicating its potential as an anticancer agent.

Author Contribution Statement

Indah Raya, Desy Kartina, and Ronald Ivan Wijaya: Conceptualization, Methodology, Supervision; Rizal Irfandi, and Eid A. Abdalrazaq: Conceptualization, Methodology, Investigation, Writing—original draft; Prihantono, Santi, Eka Pratiwi, and Andi Besse Khaerunnisa: in vitro test analysis of breast cancer: Dewi Luthfiana, Bulkis Musa, and Hasnah Natsir: molecular docking; Maming, Zaraswati Dwyana Zainuddin, and Ramlawati: molecular dynamic; Ahmad Fudholi, Andi Nilawati Usman, Unang Supratman, Maulida Mazaya and Sandi Sufiandi: Writing – review & editing, Validation.

Acknowledgements

General

We express our gratitude to Hasanuddin University's Inorganic Laboratory and Padjadjaran University's Central Laboratory for their support of this study.

Funding Statement

Grant funding for this research was provided by the Hasanuddin University Research and Community Service Institute under contract number 00323/UN4.22/PT.01.03/2023, as part of the Collaborative Fundamental Research plan for the 2023 Fiscal Year.

Ethical Declaration

Both humans and animals are not used as research participants in this study.

Conflict of Interest

The authors declare that none of the work reported in this study could have been influenced by any known competing financial interests or personal relationships.

References

- Agustiansyah P, Sanif R, Nurmaini S, et al (2021). Epidemiology and Risk Factors for Cervical Cancer, Bioscientia Medicina. *J Biomed Transl Res*, **5**, 624-31.
- Avendaño C, Menéndez J (2008). Medicinal Chemistry of Anticancer Drugs. Elsevier, Amsterdam.
- Awaluddin F, Batubara I, Wahyudi S (2021). Molecular dynamics simulation of bioactive compounds against six protein targets of Sars-Cov-2 as Covid-19 antiviral candidates. *J Kim Val*, **7**, 178-87.
- Bain C, Burton K, McGavigan C (2011). Gynaecology Illustrated 6th Edition. Elsevier, Edinburgh.
- Cardoso F, Bedard PL, Winer EP, et al (2009). International guidelines for management of metastatic breast cancer: combination vs sequential single-agent chemotherapy. *J Natl Cancer Inst*, **101**, 1174-81.
- Deswati, Suyani H, Zein R, et al (2020). Analysis Method of Anti-Cancer Drug Semustine for Chemotherapy by Cyclic Voltametry. *RJC*, **13**.
- Dorcier A, Wee H, Sandra B, et al (2006). In Vitro Evaluation of Rhodium and Osmium RAPTA Analogues: The Case for Organometallic Anticancer Drugs Not Based on Ruthenium. *Organometallic*, **25**, 4090-6.
- Durrant JD, McCammon JA (2011). Molecular dynamics simulations and drug discovery. *BMC Biol*, **9**, 71.
- Ghosh P, Saha S, Mahapatra A (2007). Mechanistic studies on the Pd-Cl cleavage of dichloro-[1-alkyl-2-(naphthylazo)imidazole] palladium(II) complexes by 8-quinolinol. *Polyhedron*, **26**, 2655-62.
- Gong C, Yao H, Liu Q, et al (2010). Markers of tumor-initiating cells predict chemoresistance in breast cancer. *PLoS One*, **5**, e15630.
- Guney G, Cecener G, Dikmen G (2018). Therapeutic Potential of BMN 673 Loaded Solid Lipid Nanoparticles in Triple Negative Breast Cancer, Conference: NANO, Kiev, Ukraine.
- Hadjiiladis N, Sletten E (2009). Metal Complexes-DNA Interactions. John Wiley and Sons, United Kingdom.
- Huang R, Wallqvist A, Covell DG (2005). Anticancer metal compounds in NCI's tumor-screening database: putative mode of action. *Biochem Pharmacol*, **69**, 1009-39.
- Irfandi R, Prihantono RI (2019). Synthesis, Characterization And Cytotoxic Activity of Zn(II) Cysteine Dithiocarbamate In Breast Cancer (MCF-7). *Int Res J Pharm*, **10**, 69-72.
- Irfandi R, Raya I, Ahmad A, et al (2022). Review on Anticancer Activity of Essential Metal Dithiocarbamate Complexes. *Indones J Chem*, **22**, 1722-36.
- Irfandi R, Raya I, Ahmad A, et al (2023). Anticancer potential of Cu(II)prolinedithiocarbamate complex: design, synthesis, spectroscopy, molecular docking, molecular dynamic, ADMET, and in-vitro studies. *J Biomol Struct Dyn*, **41**, 12938-50.
- Irfandi R, Riswandi R, Raya I, et al (2022). A New Complex Design of Fe (II) Isoleucine Dithiocarbamate as a Novel Anticancer and Antivirus against SARS-CoV-2 (COVID-19). *Asian Pac J Cancer Prev*, **23**, 3113-23.
- Irfandi R, Santi S, Raya I, et al (2022). Study of new Zn(II) Prolinedithiocarbamate as a potential agent for breast cancer: Characterization and molecular docking. *J Mol Struct*, **1252**, 132101.
- Jalili S, Maddah M, Schofield J (2016). Molecular dynamics simulation and free energy analysis of the interaction of platinum-based anti-cancer drugs with DNA. *J Theor Comput Chem*, **15**, 1650054.
- Kartina D, Wahab A, Ahmad A (2019). In Vitro Antibacterial and Anticancer Activity of Zn(II)valinedithiocarbamate Complexes. *J Phys Conf Ser*, **1341**, 1-7.
- Lancelotti P, Gómez J, Galderisi M (2017). Anticancer, Treatments and Cardiotoxicity: Mechanisms, Diagnostic, and Therapeutic Interventions. Elsevier, Amsterdam.
- Li J, Liu R, Jiang J, et al (2019). Zinc(II) Terpyridine Complexes: Substituent Effect on Photoluminescence, Antiproliferative Activity, and DNA Interaction. *Molecules*, **24**,
- Lucey BP, Nelson-Rees WA, Hutchins GM (2009). Henrietta Lacks, HeLa cells, and cell culture contamination. *Arch Pathol Lab Med*, **133**, 1463-7.
- Martínez L (2015). Automatic identification of mobile and rigid substructures in molecular dynamics simulations and fractional structural fluctuation analysis. *PLoS One*, **10**, e0119264.
- Monim-ul-Mehboob M (2013). Synthesis, Characterization and Anticancer Activity of New Gold(III) Complex with Diamine and Thione Ligands. King Fahd University of Petroleum & Minerals, Dhahran.

- Nair PC, Miners JO (2014). Molecular dynamics simulations: from structure function relationships to drug discovery. *In Silico Pharmacol*, **2**, 4.
- Nyarko E, Hanada N, Habib A, et al (2004). Fluorescence and phosphorescence spectra of Au(III), Pt(II) and Pd(II) porphyrins with DNA at room temperature. *Inorg Chim Acta*, **357**, 739-45.
- Salo-Ahen O, Alanko I, Bhadane R, et al (2021). Molecular dynamics simulations in drug discovery and pharmaceutical development. *Processes*, **9**.
- Suryoadji K, Ridwan A, Studi P, et al (2022). Vaksin HPV Sebagai Strategi Pencegahan Kanker Serviks Di Indonesia. *JIMKI*, **10**, 114-20.
- Tsuneo I (2017). Anti-Cancer Effects of Zinc (II) Ion in Tumor Formation and Growth, Proliferation, Metastasis and DNA Damage. *Degenerative Intellect Dev Disabil*, **1**, 1-8.
- Vila N, Besada P, Brea J, Loza MI, Terán C (2022). Novel Phthalazin-1(2H)-One Derivatives Displaying a Dithiocarbamate Moiety as Potential Anticancer Agents. *Molecules*, **27**.
- YASARA nd (2023). Molecular dynamics trajectory analysis for 4mbs [Internet]. [cited 2023 Apr 18]. Available from: http://www.yasara.org/mdreport/4mbs_report.html.
- Yeo C, Tiekink E, Chew J (2021). Insights into the antimicrobial potential of dithiocarbamate anions and metal-based species. *Inorganics*, **9**, 1-25.
- Zhang W, Duan Y, Wu C, et al (2003). A point-charge force field for molecular mechanics simulations of proteins based on condensed-phase quantum mechanical calculations. *J Comput Chem*, **24**, 1999-2012.



This work is licensed under a Creative Commons Attribution-Non Commercial 4.0 International License.